2.2.5
CENTRIFUGAL PUMP OIL FILM JOURNAL BEARINGS

WILBUR SHAPIRO

PRINCIPLES OF OPERATION

A journal bearing is essentially a viscous pump, and it derives load capacity by pumping the lubricant through a small clearance region. In Figure 1, the fluid is dragged along by

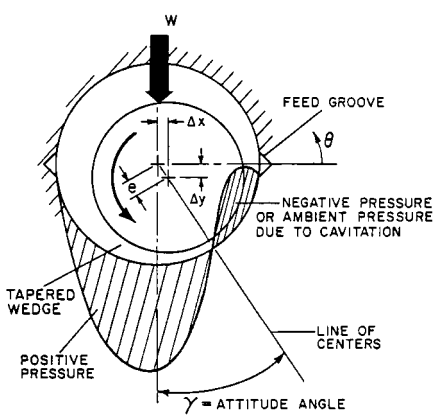

FIGURE 1 Two-groove cylindrical bearing.

the rotating journal. To generate pressure, the resistance to pumping must increase in the direction of the flow. In the figure, the journal moves to form a converging tapered clearance in the direction of the rotation or flow.

The eccentricity e is the total displacement of the journal from its concentric position. The attitude angle γ in Figure 1 is the angle between the load direction and the line of centers. Note that, because of the necessity to form a converging wedge, the displacement of the journal is not along a line that is coincident with the load vector. A positive pressure is produced in the converging region of the clearance. Downstream from the minimum film thickness, which occurs along the line of centers, the film becomes divergent. The resistance decreases in the direction of pumping, and either negative pressures occur or the air in the lubricant gasifies or cavitates and a region of atmospheric pressure occurs in the bearing area. This phenomenon is known as *fluid film bearing cavitation*. It should be clearly distinguished from other forms of cavitation that take place in pumps, such as in the impeller, for example. Here the fluid is traveling at a high velocity and the inertia forces on each fluid element dominate. Implosions occur in the impeller and can cause damage.

In a bearing, the viscous forces dominate and each fluid particle moves at a constant velocity in proportion to the net shearing forces on it. Thus, cavitation in a bearing is more of a change of the phase of the lubricant that occurs in a region of lower pressure that permits the release of entrained gases. Generally, bearing cavitation does not cause damage.

Regimes of Lubrication Whether or not a fluid film can be formed, journal rotation is dependent on several factors including the surface speed, viscosity, and load capacity. A parameter[1] is often used to determine a particular regime of lubrication, $ZN/\overline{P}$, where

Z = viscosity of lubricant, cP (Pa · s)
N = rotating speed, rpm
$\overline{P}$, = average pressure of the bearing, lb/in^2 (bar)*

A plot of the coefficient of friction versus $ZN/\overline{P}$ generally has the form shown in Figure 2. At low values of $ZN/\overline{P}$, a combination of viscosity, speed, and load places a bearing in a boundary lubricated regime where typical coefficients of friction are 0.08 to 0.14. Boundary lubrication implies intimate contact between the opposed surfaces. As the value of the parameter increases as a result of the increased speed, increased viscosity, or lowered load, there is a dramatic reduction in the coefficient of friction. In this region, there is a mixed film lubrication and the coefficient of friction varies between 0.02 and 0.08. By mixed film lubrication, it is meant that the journal is partly surrounded by a fluid film and is partly supported by rubbing contact between the opposed members. As $ZN/\overline{P}$ increases

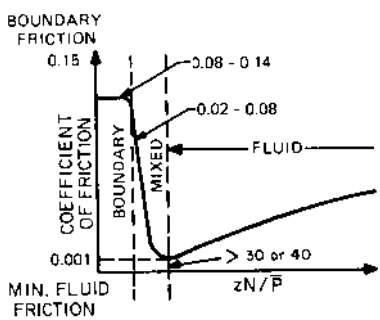

FIGURE 2 Coefficient of friction versus $ZN/\overline{P}$ (Ref. 1).

*1 bar = 10^5 Pa. For a discussion of bar, see "SI Units: A Commentary" in the front matter.

further, a situation of full fluid film lubrication prevails.

A general rule of thumb is that $ZN/\overline{P}$ should be 30 (0.44) or greater for a fluid film to be generated. Note that as $ZN/\overline{P}$ continues to increase beyond the full film demarcation, the coefficient of friction rises, but at a relatively low rate and generally remains in regions of low coefficients of friction.

EXAMPLE

$$Z = 30 \text{ cP } (0.03 \text{ Pa} \cdot \text{s})$$

$$N = 150 \text{ rpm}$$

$$\overline{P} = 200 \text{ lb/in}^2 \text{ (13.6 bar)}$$

$$\frac{ZN}{\overline{P}} = \frac{30 \times 150}{200} = 22.5$$

The bearing is not fluidborne and is operating in the mixed film regime. At what speed will the bearing become hydrodynamic? For hydrodynamic operations, $ZN/\overline{P} = 30$. Therefore,

$$N = \frac{30\overline{P}}{Z} = \frac{30 \times 200}{30} = 200 \text{ rpm}$$

THEORETICAL FOUNDATIONS

The foundation of a fluid film-bearing analysis emanates from the boundary layer theory of fluid mechanics. The governing differential equation was first formulated by Osborne Reynolds in 1886 and is known as Reynolds' equation in his honor. It has been only in the last 30 years or so that general solutions have been obtained, and this has been primarily due to the use of numerical methods applied to the digital computer. References 2 and 3 go into the details of contemporary numerical solutions and are recommended for those interested in the analytical aspects of lubrication.

Principal Assumptions Reynolds' equation can be derived from the Navier-Stokes equation of fluid mechanics, and a number of textbooks are available that comprehensively describe the derivation.[4] The primary assumptions are as follows:

- Laminar flow conditions prevail, and the fluids obey a Newtonian shear stress distribution where the shear stress is proportional to the velocity gradient.
- Inertial forces, resulting from acceleration of the liquid, are small relative to the viscous shear forces and may be neglected.
- The pressure across the film is constant since the fluid films are so thin.
- The height of the fluid film is small relative to other geometric dimensions, and so the curvature of the fluid film can be ignored.
- The viscosity of the liquid remains constant. In most cases, this is a reasonable assumption since it has been repeatedly demonstrated that, if the average viscosity is used, little error is introduced and the complexity of the analysis is considerably reduced.

Derivaton of Reynold's Equation of Lubrication Assume that the rotating journal has a peripheral velocity U. Consider an elemental volume in the clearance space of the bearing and establish equilibrium (see Figure 3). Note that since inertial forces are neglected, the volume is in equilibrium by the pressure and shear forces acting upon it, so there is no acceleration. As shown in Figure 4, p is the pressure and τ is the shear stress acting upon the volume. Summing forces in the x direction

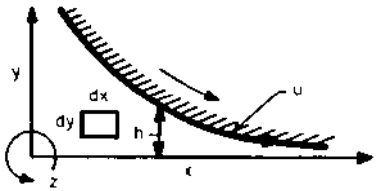

FIGURE 3 Fluid control volume.

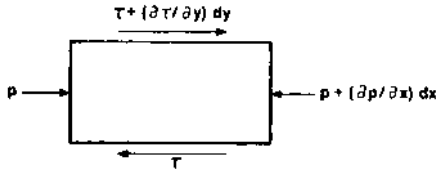

FIGURE 4 Force equilibrium on fluid element.

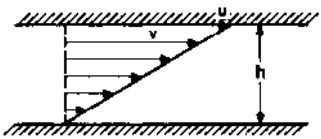

FIGURE 5 Laminar velocity distribution across film.

$$p\,dy\,dz - \left(p + \frac{\partial p}{\partial x}\,dx\right)dy\,dz - \tau\,dx\,dz + \left(\tau + \frac{\partial \tau}{\partial y}\,dy\right)dx\,dz = 0 \tag{1}$$

$$-\frac{\partial p}{\partial x}\,dx\,dy\,dz + \frac{\partial \tau}{\partial y}\,dx\,dy\,dz = 0$$

or

$$\frac{\partial p}{\partial x} = \frac{\partial \tau}{\partial y} \tag{2}$$

For a Newtonian fluid in a laminar flow, the shear stress is directly related to the velocity gradient with the proportionality constant being the absolute viscosity μ (see Figure 5):

$$\tau = \mu \frac{dv}{dy} \tag{3}$$

$$\frac{\partial \tau}{\partial y} = \mu \frac{\partial^2 v}{\partial y^2}$$

where ν is the fluid velocity. Substituting Equation 3 into Equation 2, we obtain

$$\frac{\partial p}{\partial x} = \mu \frac{\partial^2 v}{\partial y^2} \tag{4}$$

Integrating with respect to y twice produces the following equation:

$$v = \frac{1}{\mu}\,\frac{\partial p}{\partial x}\,\frac{y^2}{2} + C_1 y + C_2 \tag{5}$$

where C_1 and C_2 are constants of integration. The boundary conditions are

$$v = 0, y = 0 \text{ and} \tag{6}$$

$$v = u, y = h$$

Substituting the boundary conditions of Equation 6 into Equation 5 results in the following expression for v:

$$v = \frac{1}{2\mu}\,\frac{\partial p}{\partial x}\,(y^2 - h^2 y) + \frac{uy}{2} \tag{7}$$

The velocity in the z direction would be similar, except that the surface velocity term would be omitted because no surface velocity exists in the z direction. In addition, the pressure gradient would be with respect to z.

Now let us consider the flow across the film due to this velocity. Note that Equation 7 is the velocity computed in the x direction, which is in the direction of rotation of the journal:

$$q_x = \int_0^h v_x \, dy = \int_0^h \left[\frac{1}{2\mu} \frac{\partial p}{\partial x} (y^2 - h^2 y) + \frac{uy}{2} \right] dy \tag{8}$$

After integrating,

$$q_x = -\frac{1}{12\mu} \frac{\partial p}{\partial x} h^3 + \frac{1}{2} uh \tag{9}$$

Note that q_x is the flow per unit width across the film. The flow in the axial direction is

$$q_z = -\frac{1}{12\mu} \frac{\partial p}{\partial z} h^3 \tag{10}$$

Now let us consider a flow balance through an elemental volume across the film (see Figure 6). The net outflow through the volume equals the net reduction in volume per unit time:

$$\left(q_x + \frac{\partial q_x}{\partial x} dx \right) dz - q_x \, dz + \left(q_z + \frac{\partial q_z}{\partial z} dz \right) dx - q_z \, dx = -\frac{\partial h}{\partial t} dx \, dz \tag{11}$$

Thus, this gives us

$$\frac{\partial q_x}{\partial x} + \frac{\partial q_z}{\partial z} = -\frac{\partial h}{\partial t} \tag{12}$$

Substituting Equations 9 and 10 into Equation 12, we obtain

$$-\frac{\partial}{\partial x} \left(\frac{1}{12\mu} h^3 \frac{\partial p}{\partial x} \right) - \frac{\partial}{\partial z} \left(\frac{1}{12\mu} h^3 \frac{\partial p}{\partial z} \right) = -\frac{\partial h}{\partial t} - \frac{u}{2} \frac{\partial h}{\partial x} \tag{13}$$

and the final equation becomes

$$\frac{\partial}{\partial x} \left(\frac{h^3}{\mu} \frac{\partial p}{\partial x} \right) + \frac{\partial}{\partial z} \left(\frac{h^3}{\mu} \frac{\partial p}{\partial z} \right) = 6\mu \frac{\partial h}{\partial x} + 12 \frac{\partial h}{\partial t} \tag{14}$$

Equation 14 is the general form of Reynolds' equation used for laminar, two-dimensional lubrication problems.

Reynolds' equation is a flow balance equation. The left-hand side represents pressure-induced flows in the x and z directions through the differential element. The first term on the right-hand side represents the shear flow of the fluid induced by the surface velocity of the journal u. Note that this term contains the derivative of clearance with respect to distance. If this term is zero, then there is zero pressure produced by hydrodynamic action,

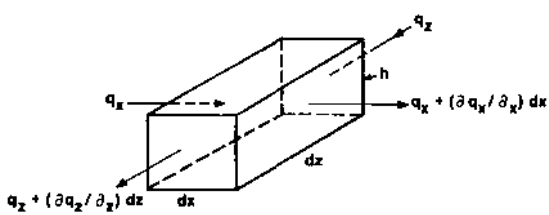

FIGURE 6 Flow balance across control volume.

and the term ∂h/∂x is the mathematical representation of the tapered wedge. The second term on the right-hand side refers to a time rate of change of the film thickness, which can be translated to a normal velocity of the center of the journal. It produces pressure by a fluid velocity normal to the bearing surfaces that attempts to squeeze fluid out of a restricted clearance space. This phenomenon is called the squeeze film effect in bearing terminology. Since it is proportional to the velocity of the center of the journal, it is the phenomenon that produces viscous damping in a bearing.

The solution to Reynolds' equation (refer to Equation 14) provides the pressure at all points in the bearing. The application of the digital computer has enabled a rapid solution of Reynolds' equation over a grid network representing the bearing area.[2,3]

Once the pressures have been obtained, a numerical integration is applied to determine the performance parameters (in other words, the load capacity):

$$w = \int\int prd\theta\, dr \tag{15}$$

The flow across any circumferential line is

$$q_\theta = \oint\left(-\frac{1}{12\mu}\,\frac{\partial p}{r\partial\theta}\,h^3 + \frac{1}{2}\,uh\right) dz \tag{16}$$

The flow across any axial line is

$$qz = \oint\left(-\frac{1}{12\mu}\,\frac{\partial p}{\partial z}\,h^3\right) rd\theta \tag{17}$$

The viscous frictional moment is obtained by integrating the shear stress over the area and can be shown to be

$$M_f = \int\int\left[\frac{1}{r}\,\frac{\partial p}{\partial\theta}\,\frac{h}{2} + \frac{\mu r\omega}{h}\right] r^2 d\theta\, dz \tag{18}$$

where ω = journal surface speed, rad/s.

Typical computer program output includes the following:

- Pressure distribution throughout the grid network
- Load capacity
- Side leakage and carryover flows
- Viscous power losses
- Righting moments due to misalignments
- Attitude angles
- Cross-coupled spring and damping coefficients due to displacements and velocity perturbations of the journal center
- Clearance distribution

Turbulence Equation 14 is for laminar conditions. For very high speed bearings, operations beyond the turbulent regime may occur and Reynolds' equation must be modified. The turbulent theory has been developed, and the literature on this topic can enable performance predictions for turbulent bearings.[5,6]

The onset of turbulence is determined by examining the bearing's Reynolds number, which is the ratio of inertia to viscous forces and is defined as

$$Re = \frac{\rho u h}{\mu} \tag{19}$$

where Re = Reynolds number
ρ = fluid density, lb · s²/in⁴ (kg/m³)
u = surface velocity, in/s (m/s)
h = local film thickness, in (m)
μ = viscosity, lb · s/in² (Pa · s)

A reasonable approximation is to use the concentric clearance c for h. In terms of N rpm and journal diameter D, the Reynolds number is

$$Re = \rho \frac{\pi DN}{60} \frac{c}{\mu} \tag{20}$$

The criterion for turbulence in journal bearings is that $Re \geq 1000$.

EXAMPLE As an example, consider the following:

Journal diameter $D = 5$ in (127 mm)
Bearing length $L = 5$ in (127 mm)
Radial clearance $c = 0.0025$ in (0.064 mm)
Operating speed $N = 5000$ rpm
Lubricant viscosity $\mu = 2 \times 10^{-6}$ lb · s/in² (14×10^{-3} Pa · s)
Lubricant density $\rho = 7.95 \times 10^{-5}$ lb · s²/in⁴ (8.66×10^{-11} kg · s²/mm⁴)

$$Re = \rho \frac{\pi DN}{60} \frac{c}{\mu}$$

$$= 7.95 \times 10^{-5} \times \frac{\pi \times 5 \times 5000}{60} \times \frac{0.0025}{2 \times 10^{-6}} = 130$$

Thus, the bearing is operating in the laminar regime. To become turbulent (assuming constant viscosity), the operating speed would have to increase to approximately 38,500 rpm.

The example cited is for a relatively high-speed, oil-lubricated bearing for pump applications. In general, most pump bearings operate in the laminar regime. Exceptions might occur when water is used as tbe lubricant because it its much less viscous than oil.

Evaluation of Frictional Losses It is often desirable to obtain a quick estimate of viscous drag losses that the journal bearings produce. If we consider shear forces again, we return to the laminar flow equation:

$$F = \mu A \frac{\mu}{h} \tag{21}$$

where F = viscous shear force, lb (N)
μ = viscosity, lb · s/in² (Pa · s)
A = surface area, in² (m²)
u = journal velocity, in/s (m/s)
h = film thickness, in (m)

To obtain friction, we multiply both sides of Equation 21 by the journal radius R. Then the viscous frictional moment is

$$M = \mu A R \frac{u}{h}$$

The frictional horsepower loss is

$$FHP = \frac{NM}{63{,}000}$$

where N = rotating speed, rpm
M = moment, lb · in (N · m)

Also

A = surface area of bearing = πDL, in^2 (m^2)

u = surface speed = $\frac{\pi DN}{60}$ in/s (m/s)

Substituting, we obtain

$$FHP = \frac{\mu L D^3 N^2}{766{,}000h} \tag{22}$$

In obtaining approximate losses for estimation purposes, the concentric clearance c is substituted for the local film thickness h.

If we consider the previous example where $D = 5$ in (127 mm), $L = 5$ in (127 mm), $c = 0.0025$ in (0.064 mm), $N = 5000$ rpm, and $\mu = 2 \times 10^{-6}$ lb · s/in^2 (14×10^{-3} Pa · s), the horsepower loss is

$$FHP = \frac{(2 \times 10^{-6})(5)(5)^3(5000)^2}{(766{,}000)(0.0025)} = 16.32 \text{ hp}$$

Note that for thrust bearings, the frictional horsepower loss is

$$FHP = \frac{\mu N^2}{h} \frac{OD^4 - ID^4}{6.127 \times 10^6} \tag{23}$$

where OD = outside diameter
ID = inside diameter

A general rule of thumb is that the frictional horsepower in a thrust bearing is approximately twice that in a journal bearing.

BEARING TYPES

Cylindrical Bearing The most common type of journal bearing is the plain cylindrical bushing shown schematically in Figure 1. It can be split and have lubricating feed grooves at the parting line. A ramification is to incorporate axial grooves to enable better cooling and to improve whirl stability (described in more detail below in the discussion of cylindrical bearings with axial grooves). The principle advantages of cylindrical bearings are (1) simple construction and (2) a high-load capacity relative to other bearing configurations.

This type of bearing also has several disadvantages:

- *Whirl Instability:* This is prone to subsynchronous whirling at high speeds and also at low loads. Whirling is an orbiting of the journal (shaft) center in the bearing, a motion that is superimposed upon the normal journal rotation. The orbital frequency is approximately half the rotating speed of the shaft. The expression *half-frequency whirl* is commonly used. The reason for the occurrence of this whirl and more details concerning bearing dynamics are presented in the section on bearing dynamics.
- *Viscous Heat Generation:* Because of the generally large and uninterrupted surface area of this bearing, it generates more viscous power loss than some other types.

- *Contamination:* The cylindrical bearing is more susceptible to contamination problems than other types because contaminants that are dragged in at the leading edge of the bearing cannot easily dislodge because of the absence of grooves or other escape paths.

The advantages of simplicity and load capacity make the plain journal a leading candidate for most applications, but performance should be carefully investigated for whirl instability and potential thermal problems. Cylindrical bearings are generally used for medium-speed (500 in/s [200 mm/sec] surface speed) and medium- to heavy-load applications (250 to 400 lb/in^2 [17 to 28 bar] on a projected area).

Cylindrical Bearing with Axial Grooves A typical configuration of this type of bearing is a plain cylindrical bearing with four equally spaced longitudinal grooves extending most of the way through the bearing. Usually, a slight land area exists at either end of the groove to force the inlet flow to each groove into the bearing clearance region (see Figure 7), rather than out the groove ends. This configuration is a little less simple than the plain cylindrical bearing, and because the grooves consume some land area, this configuration has less load capacity than the plain bushing. Since oil is fed into each of the axial grooves, this bearing requires more inlet flow but also will run cooler than the plain bushing. The grooves act as convenient outlets for any contaminants in the lubricant, and thus the grooved bearing can tolerate more contamination than the plain cylindrical bearing.

In general, this bearing can be considered as an alternate to a plain bearing if the former can correct a whirl or overheating problem.

Elliptical and Lobe Bearings Elliptical and lobe bearings have noncircular geometries. Figure 8 shows two types of three-lobe bearings with the clearance distribution exaggerated so that the lobe geometry is easily discernible. An elliptical bearing is simply a two-lobe bearing with the major axis along the horizontal axis.

The lobe bearing shown in Figure 8a is a symmetric lobe bearing where the minimum concentric clearance occurs in the center of each lobed region. Thus, at the leading edge region, a converging clearance produces positive pressure, but downstream from the minimum film thickness, a divergent film thickness distribution can be found with resulting negative, or cavitation, pressures.

The canted lobe in Figure 8b, on the other hand, generally develop positive pressure throughout the lobe because the bearing is constructed with a completely converging film thickness in each lobed region. This design has excellent whirl resistance (superior to that of the symmetric lobe bearing) and a reasonably good load capability. A 2:1 ratio between leading and trailing edge concentric clearance is generally a reasonable compromise with respect to performance.

Elliptical and lobe bearings are often used because they provide better resistance to whirls than cylindrical configurations. They do so because they have multiple load-producing pads that assist in preventing large-attitude angles and cross-coupling (see the section on bearing dynamics). Elliptical and lobe bearings are generally used for high-speed, low-load applications where whirls might be a problem.

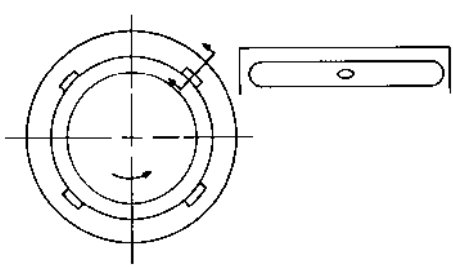

FIGURE 7 Cylindrical bearing with axial grooving.

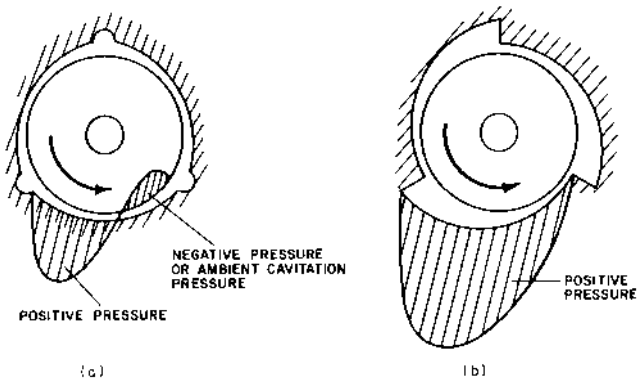

FIGURE 8 (a) symmetric lobe bearing and (b) canted lobe bearing.

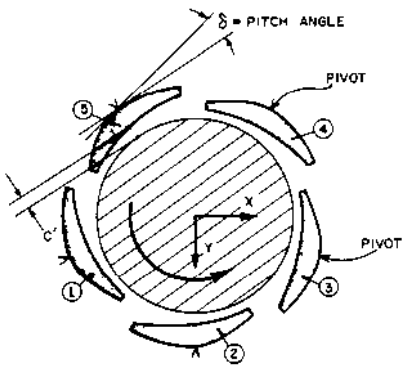

FIGURE 9 Five-pad tilting pad bearing.

Elliptical, or two-lobe, bearings generally have poor horizontal stiffness because of the large clearances along the major diameter of the ellipse. The split elliptical configuration, however, is easier to manufacture than the other types because it is two cylindrical bearing halves with material removed along the parting line. Lobe bearings are usually clearance- and tolerance-sensitive. The other types of lobe bearings are complicated to manufacture.

Tilting-Pad Bearings Tilting-pad bearings are used extensively, especially in high-speed applications, because of their whirl-free characteristics. They are the most whirl-free of all bearing configurations.

An important geometric variable for tilting-pad bearings is the preload ratio, defined as shown in Figure 9.

The preload ratio equals

$$\text{Preload ratio} = PR = \frac{c - c'}{c} = 1 - \frac{c'}{c} \tag{24}$$

where c = machined clearance
c' = concentric pivot film thickness

The variable c' is an installed clearance and is dependent upon the radial position of the pivot. Figure 10 displays two pads. Pad 1 has been installed such that the preload ratio

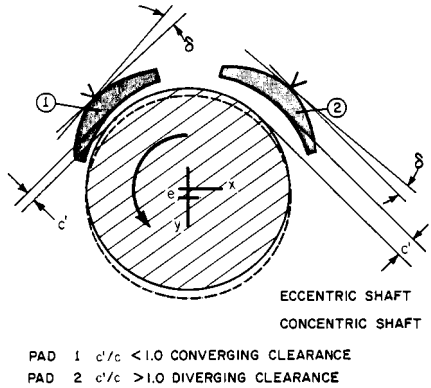

FIGURE 10 Tilting-pad bearing preload.

is less than one. For pad 2, the preload ratio is one. The solid line represents the position of the journal in the concentric position. The dashed portion of the journal represents its position when a load is applied to the bottom pads (not shown). Pad 1 is operating with a good converging wedge, even though the journal is moving away from it. Pad 2, on the other hand, is operating with a completely diverging film, which means that it is totally unloaded. Thus, bearings with installed pad preload ratios of one or greater will operate with unloaded pads, which reduces overall stiffness of the bearing and results in a deterioration of stability because the unloaded pads do not aid in resisting cross-coupling influences. In the unloaded position, they are also subject to flutter instability and to a phenomenon known as *leading edge lockup,* where the leading edge is forced against the shaft and is maintained in that position by the frictional interaction of the shaft and the pad. This is especially prevalent in bearings that operate with low-viscosity lubricants, such as gas or water bearings. Thus, it is important to design bearings with preload, although for manufacturing reasons it is common practice to produce bearings without preload.

Tilting-pad bearings have some other characteristics that are both positive and negative:

- They are not as clearance-sensitive as most other bearings.
- Because the pads can move, they can operate safely at a lower minimum film thickness than other bearings.
- They do not provide as much squeeze film damping as rigid configurations.
- Generally, they are more expensive than other bearings.
- For high-speed applications, their pivot contacts can be subjected to fretting corrosion.

Hybrid Bearings A hybrid bearing, schematically shown in Figure 11, derives a load capacity from two sources: (1) the normal hydrodynamic pressure generation and (2) an external high-pressure supply that introduces oil into recesses machined into the bearing surface via restrictors (orifices or capillaries upstream of the recesses). External pressure significantly enhances load capacity. Also, these bearings have excellent low- or zero-speed load capabilities. They are sometimes used as startup devices to lift off the rotor. When self-sustaining hydrodynamic speeds are attained, the external pressure is shut off. The characteristics of externally pressurized, or hybrid, bearings include the following:

- High load and stiffness capabilities
- An external flow that assists in cooling

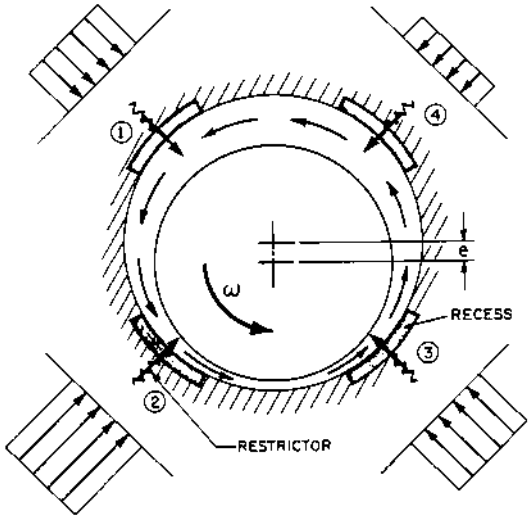

FIGURE 11 Cross-coupling influences in hybrid bearings.

- Their clearances and tolerances are generally more liberal than in hydrodynamic bearings
- They require external fluid-supply systems
- They are applied when there is not a sufficient generating speed or when a high-load capacity and stiffness are required
- They are sometimes applied to prevent a whirl, but rotational speeds can unbalance recess pressures, introduce cross coupling, and promote a whirl.

STEADY STATE PERFORMANCE

Computer-generated performances have been obtained for most of the bearing types previously discussed. Information has been plotted in a nondimensional format so that no restrictions exist on operating conditions, lubricant properties, and so on. Use of the charts will be subsequently demonstrated by numerical example.

Viscosity One of the key parameters in determining the performance of a bearing is the lubricant viscosity. Viscosity characteristics of commonly used Society of Automotive Engineers (SAE) grades of oil are shown in Figure 12. The units of viscosity are *microreyns*, where the reyn has the units of $\text{lb} \cdot \text{s/in}^2$ and comes from the ratio of shear stress to the velocity gradient across the film, as indicated by Equation 21. Other units of viscosity are *centipoises*, *Saybolt seconds universal* (SSU), and *centistokes*. The conversion factors are as follows:

$$\mu(\text{reyns}) = Z \times 1.45 \times 10^{-7} \tag{25}$$

$$\nu(\text{centistokes}) = 0.22\,(\text{SSU}) - \frac{180}{\text{SSU}} \tag{26}$$

$$Z(\text{centiposes}) = \nu(\text{centistokes}) \times \text{SG (sp. gr.)} \tag{27}$$

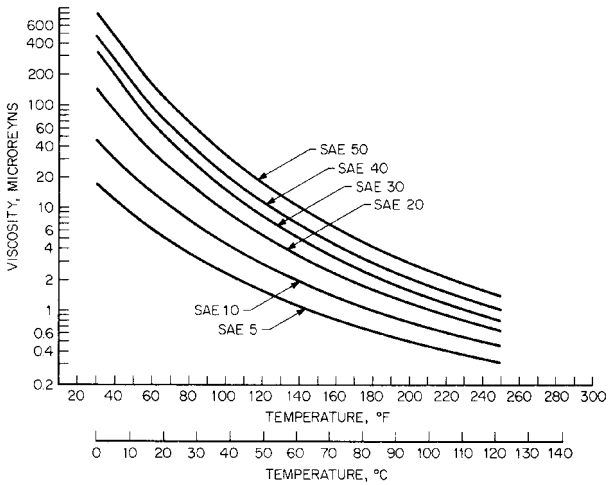

FIGURE 12 Viscosity characteristics for SAE oil grades.

Performance Curves Performance plots have been generated for the following types of bearings:

- *Two-groove cylindrical bearings*
- *Symmetric three-lobe bearings:* Each lobe is offset such that in the concentric position the minimum film thickness in the center of each lobed region is half the machined clearance c (see definition following). The pads are each 110° in the angular extent.
- *Canted three-lobe bearing:* The lobing is canted such that in the concentric position the leading edge clearance was twice the trailing edge and the trailing edge film thickness (minimum) in the concentric position was $0.5c$ where c equals the machined clearance. The pads are each 110° in the angular extent.
- *Tilting-pad bearing:* The tilting-pad bearing that information is obtained for is a five-pad bearing with a 60° pad and a preload ratio of 30 percent.

Two length/diameter ratios are examined for each type of bearing: $L/D = 0.5$ and 1.0. The definition of the nondimensional parameters is as follows:

$$W = \text{nondimensional load parameter} = wc^2/6\mu\omega RL^3 \tag{28}$$

$$P = \text{nondimensional viscous power loss parameter} = 1100cp/\mu(\omega RL)^2 \tag{29}$$

$$Q = \text{nondimensional flow parameter} = 2q/0.26\omega RLc \tag{30}$$

$$HM = \text{nondimensional minimum film thickness} = h_M/c \tag{31}$$

where w = bearing load capacity, lb (N) and
c = reference clearance (machined clearance = radius of bearing − radius of shaft), in (mm)
μ = absolute viscosity, reyns (lb · s/in^2) (cP)
ω = shaft or journal rotational speed rad/s
R = shaft radius, in (mm)
L = bearing length, in (mm)
p = viscous power loss, hp (kW)
q = flow, gpm (m^3/h)

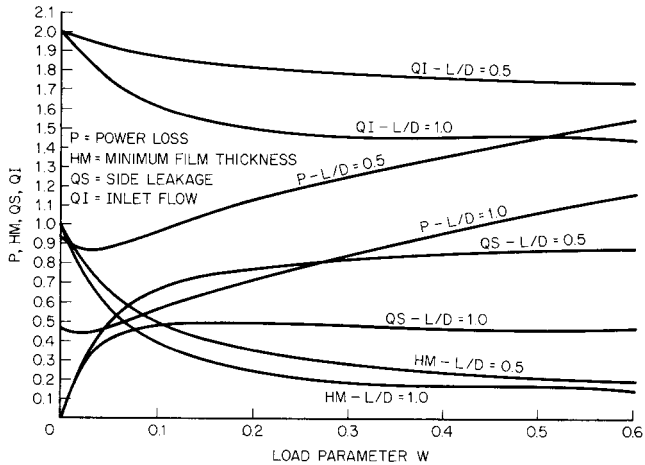

FIGURE 13 Performance characteristics for two-groove cylindrical bearings.

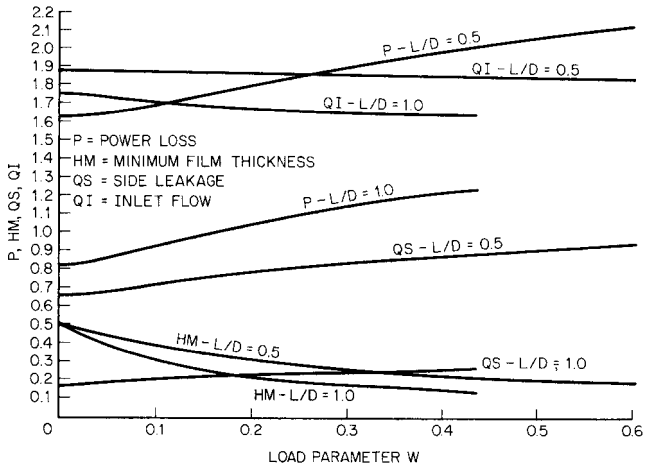

FIGURE 14 Performance characteristics for three-lobe bearings.

q_i = inlet flow to the leading edge of bearing (for multipad bearings, equals the sum of inlet flow to each pad), gpm (m^3/h)
q_s = side leakage flow or flow out of the bearing ends (for multipad bearings, equals the sum of side leakage flow of each pad), gpm (m^3/h)
h_M = minimum film thickness in bearing, in (mm)

Performance curves are shown in Figures 13 through 17.

At times, the nondimensional data can be confusing and lead to erroneous judgments. For example, the nondimensional power loss P is greater for an L/D equal to 0.5 than for an L/D equal to 1.0. However, when the dimensional value of the power loss is being computed, the nondimensional value is multiplied by L^2. Therefore, the power loss for the L/D

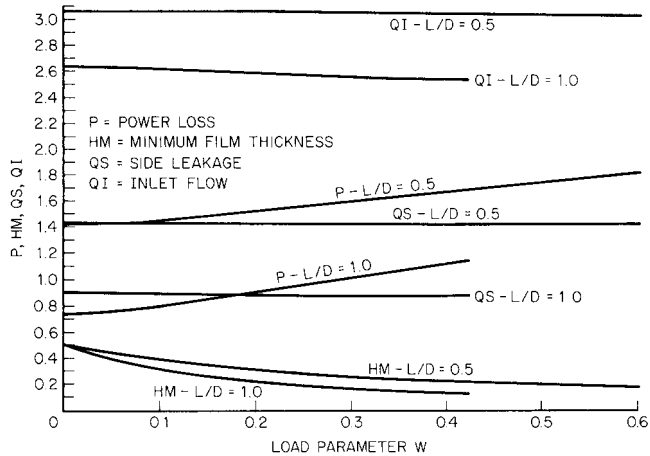

FIGURE 15 Performance characteristics for canted three-lobe bearings.

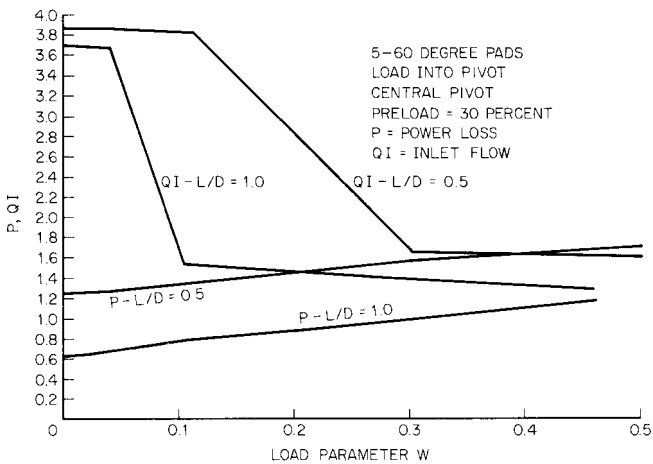

FIGURE 16 Performance characteristics for tilting-pad bearings.

equal to 1.0 will be, as expected, greater than for the L/D equal to 0.5. If the reader uses the data as presented, the dimensional information will prove consistent.

To make comparisons among the bearings, using the nondimensional data is not strictly proper because there may be slight inconsistencies in preloads, the bearings will not be operating at the same average viscosity, and so on. Subsequently, dimensional data derived from the performance curves will be compared, but comparisons of the nondimensional information will provide an indication of performance parameters among the bearings. Comparisons have been made at equal values of the load parameter W and the results are shown in Table 1.

Comparisons of the different bearing types should be made only at the same L/D ratio because of the anomalies (discussed above) of nondimensional parameters that occur at

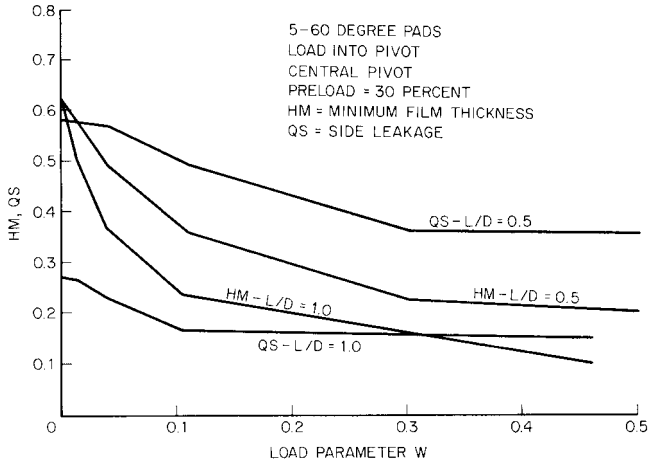

FIGURE 17 Performance characteristics for tilting-pad hearings.

TABLE 1 Comparative Results of Bearing Types at $W = 0.2$

	$L/D = 0.5$				$L/D = 1$			
Bearing type	*P*	*HM*	*QS*	*QI*	*P*	*HM*	*QS*	*QI*
Two-groove cylindrical	1.13	0.36	0.78	1.81	0.72	0.25	0.50	1.50
Three-lobe	1.80	0.32	0.79	1.85	1.05	0.22	0.22	1.65
Canted three-lobe	1.52	0.31	1.42	3.30	0.91	0.22	0.90	2.58
Tilting-pad	1.50	0.30	0.44	2.82	0.90	0.20	0.16	1.50

QI = nondimensional inlet flow = $2qi/0.26\ wRLc$
QS = nondimensional side leakage flow = $2q_s/0.26\ wRLc$

different L/D ratios. If we assume that all the reference variables that go into the nondimensional parameters are identical, we can establish the following conclusions:

- The two-groove cylindrical hearing has the highest film thickness and thus the highest load capacity.
- The symmetric three-lobe bearing has the highest power loss.
- The canted three-lobe bearing has the greatest flow requirements.

Note that these comparisons were made on the basis of steady-state performances only. The major reason for applying lobe and tilting-pad bearings is to avoid dynamic instabilities.

Heat Balance Performance is based upon the assumption of a uniform viscosity in the fluid film. Since the viscosity is a strong function of temperature and since the temperature rise of the lubricant due to viscous heat generation is not known a priori, an iterative procedure is required to determine the average viscosity in the film. To determine an average viscosity, there must be a simplified heat balance in the film. The assumption is made that all the viscous heat generated in the film is absorbed by the lubricant as it flows through the film and produces a temperature rise.

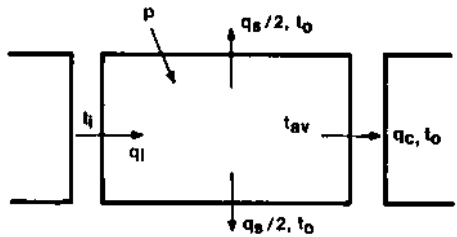

FIGURE 18 Heat balance in a fluid film.

Figure 18 shows a developed view of the bearing surface and the parameters involved with conducting the heat balance. The lubricant enters a pad or bearing at the leading edge with an inlet flow q_i and an inlet temperature t_i. As the lubricant enters the bearing surface and flows through it, the lubricant is exposed to a viscous shear, which adds heat to the fluid. In Figure 18, the viscous shear is indicated as a power input p. Some of the fluid flows out of the sides of the bearing, represented by $q_s/2$, and some of the fluid, q_c, is carried either over to the grooving of the next pad or back to the inlet groove for a single pad bearing.

Although the fluid temperature, and thus the viscosity, changes along the length of the pad, it is assumed that the temperature in the film increases to some value t_o for both the side leakage and carry-over fluids. Then the heat balance is conducted as follows:

Heat added to a fluid by a viscous shear equals heat absorbed by the fluid.

$$\begin{gathered}\text{Heat added to fluid by viscous shear} = \text{heat absorbed by fluid} \\ pJ = q_s\rho C_p(t_o - t_i) = q_c\rho C_p(t_o - t_i) = (q_s + q_c)\rho C_p(t_o - t_i)\end{gathered} \tag{32}$$

Since by continuity of flow,

$$q_i = q_s + q_c \tag{33}$$

$$pJ = q_i\rho C_p\Delta t \tag{34}$$

$$\Delta t = \frac{pJ}{q_i\rho C_p} \tag{35}$$

where p = viscous heat generation, hp
J = heat equivalent constant = 0.7069 Btu/hp · s (J/kg · s)
ρ = specific weight of flow, lb/in^3 (kg/m^3)
C_p = specific heat of fluid, Btu/lb · °F (J/kg · °C)
q_i = bearing inlet flow, in^3/s (mm^3/s)
Δt = temperature rise, °F (°C)

If q_i is in gallons per minute [(1 in^3/s = 0.26 gpm) = 16.39 cm^3/s],

$$\Delta t = \frac{0.7069(0.26)p}{q_i\rho C_p} = \frac{0.1838p}{q_i\rho C_p} \tag{36}$$

Before proceeding to a sample problem, a word about the flows q_i and q_s, and the general heat balance philosophy. The flow required by the bearing to prevent starvation is q_i. The minimum make-up flow, or the flow that is lost from the ends of the bearing, is the side leakage q_s. Theoretically then, the only flow that need be supplied to the bearing is q_s. However, if this were true, then the heat balance formulation would require another balance between the carry-over flow q_c at some temperature t_o and the make-up flow q_s coming into the pad at temperature t_i. It would be found that, if we supplied only q_s to the bearing, excessive temperatures would result. In most instances, the amount of flow supplied to a bearing exceeds both the inlet flow and the side leakage flow by a significant

margin. Designers often determine the flow to be supplied to a bearing system by a bulk temperature rise of the total flow entering the inlet pipe and exiting the exhaust pipe. Thus, the entire bearing is treated as a black box, and the total flow q_T to the bearing system for a given bulk temperature rise Δt_t is

$$q_T = \frac{pJ}{\rho C_p \Delta t_t} \tag{37}$$

Normally, Δt_t is selected between 20 and 40°F. Since q_T will exceed q_i, not all the flow will enter the film. Some will surround the bearing or flow through the feed groove and act as a cooling medium for heat transfer through the bearing walls or for cooling the fluid that does enter the bearing surface q_i.

EXAMPLE This example demonstrates the use of the design curves and how to perform a simplified heat balance in a bearing analysis.
In this example, we know these values:

Bearing type: two-groove cylindrical
Bearing length $L = 3$ in (76 mm)
Bearing diameter $D = 6$ in (152 mm)
$L/D = 0.5$
$N = 1800$ rpm; $\omega = 1800 \times \pi/30 = 188.5$ rad/s
Bearing load $\omega = 6000$ lb (2721 kg)
Inlet temperature $t_i = 120$°F (49°C)
Lubricant = SAE 20
Bearing radial clearance $c = 0.003$ in (0.076 mm)

NOTE: A general rule of thumb is that $c/R = 0.001$.
Assume an average lubricant temperature of 130°F − μ (SAE 20 at 130°F) = 4.5×10^{-6} reyn (lb · s/in^2) (31×10^{-3} Pa · s)

$$\rho = 0.0307 \text{ lb/in}^3 (849.7 \text{ kg/m}^3) \text{ (average value for most oils)}$$
$$C_p = 0.5 \text{Btu/lb} \cdot \text{F°} \ (2093 \text{ J/kg} \cdot \text{C°}) \text{ (average value for most oils)}$$

Compute the following:

$$W = \frac{wc^2}{6\mu\omega RL^3} = \frac{(6000)(0.003^2)}{(6)(4.5 \times 10^{-6})(188.5)(3)(3^3)} = 0.1309$$

From Figure 13 and Equation 29,

$$P = 1.0 = \frac{1100cp}{\mu(\omega RL)^2}$$
$$P = \frac{(1)(4.5 \times 10^{-6})(188.5 \times 3 \times 3)^2}{(1100)(0.003)} = 3.92 \text{ hp } (2.95 \text{ kW})$$

From Figure 13 and Equation 30,

$$Q_I = 1.85 = \frac{2q_i}{0.26\omega RLC}$$
$$q_i = \frac{(1.85)(0.26)(188.5)(3)(3)(0.003)}{2} = 1.224 \text{ gpm } (4.63 \text{ l/min})$$

From Equation 36,

$$\Delta t = \frac{0.1838p}{q_i \rho C_p} = \frac{(0.1838)(3.92)}{(1.224)(0.0307)(0.5)} = 38.35\ \text{F°}\ (21.3\ \text{C°})$$

$$t_{av} = \frac{t_i + (t_i + \Delta t)}{2} = \frac{2t_i + \Delta t}{2} = \frac{(2)(120) + 38.85}{2} = 139.2°\text{F}\ (59.6°\text{C})$$

The assumed t_{av} of 130°F was apparently not high enough and therefore we must repeat the calculations with a higher value of assumed t_{av}. Assume $t_{av} = 138°\text{F}$, $\mu = 3.8 \times 10^{-6}$ lb · s/in^2 (26.2×10^{-3} Pa · s) and repeat the calculations:

$$W = \frac{5.8945 \times 10^{-7}}{\mu} = 0.1552$$

$$P = 1.08 = (1.1466 \times 10^{-6})\left(\frac{p}{\mu}\right)$$

$$p = \frac{(1.08)(3.8 \times 10^{-6})}{1.1466 \times 10^{-6}} = 3.579\ \text{hp}\ (2.67\ \text{kW})$$

$$QI = 1.83 = \frac{q_i}{0.6616}$$

$$q_i = 1.211\ \text{gpm}\ (4.58\ \text{l/min})$$

$$\Delta t = 11.974\,\frac{p}{q_i} = \frac{(11.974)(3.579)}{1.211} = 35.38\ \text{F°}\ (19.65\ \text{C°})$$

$$t_{av} = \frac{(2)(120) + 35.38}{2} = 137.7°\text{F}\ (58.7°\text{C})$$

For all practical purposes, these equal the assumed value of $t_{av} = 138°\text{F}$ (58.9°C).

In conducting the iterative procedure for determining the average fluid temperature, it is sometimes helpful to plot points on a viscosity chart. Referring to Figure 19, suppose

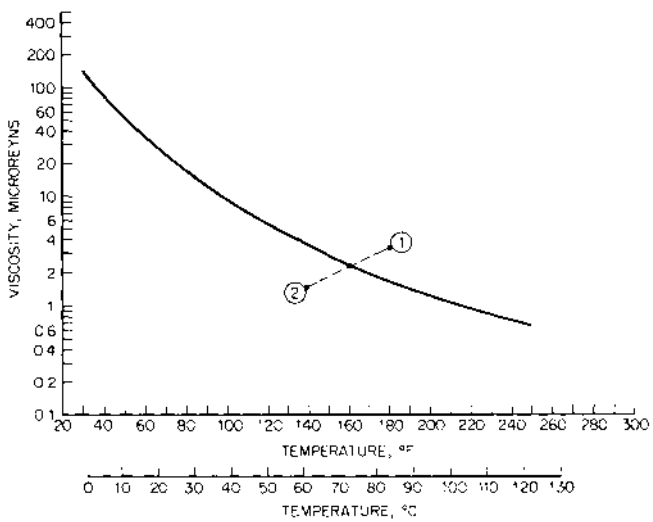

FIGURE 19 Graphical determination of average viscosity for SAE 20 oil.

point 1 is the resultant average viscosity and temperature of the initial guess and point 2 represents the result of the second guess. Then, by drawing a straight line between points 1 and 2 and establishing where it intersects the lubricant viscosity curve, we can determine the convergence to the proper result of average viscosity and temperature.

Now that we have convergence, we can determine the remaining variables, which are the minimum film thickness H_M and side leakage Q_S from Figure 13:

$$HM = 0.41 = \frac{h_M}{c}$$

$$h_M = (0.41)(0.003) = 0.00123 \text{ in } (0.031 \text{ mm})$$

$$QS = 0.74 = \frac{2q_s}{0.26\omega RLC} = \frac{q_s}{0.6616}$$

$$q_s = (0.6616)(0.74) = 0.490 \text{ gpm } (1.85 \text{ l/min})$$

A summary of the total bearing performance is as follows:

Load ω = 6000 lb (2721 kg)
Minimum film thickness h_M = 0.00123 in (0.031 mm)
Viscous power loss ρ = 3.579 (2.669 kW)
Inlet flow q_i = 1.211 gpm (4.58 l/min)
Side leakage q_s = 0.490 gpm (1.85 l/mm)
Fluid temperature rise Δt = 35.38°F (19.65°C)

We can repeat the same calculation for the other types of bearings, using Figures 14 through 17. The results are shown in Table 2.

The two-groove cylindrical bearing operates with the highest film thickness. The symmetric three-lobe has the lowest film thickness and highest temperature rise. It appears that, on the basis of steady-state performance, manufacture, and cost, the two-groove cylindrical bearing is the best choice.

BEARING DYNAMICS[7]

Fluid film bearings can significantly influence the dynamics of rotating shafts. They are a primary source of damping and thus can inhibit vibrations. Alternatively, they provide a

TABLE 2 Comparative Bearing Performance

Bearing type	Δt, °F (°C)	t_{av}, °F (°C)	p, hp	q_i, gpm (cm^3/s)	q_s, gpm (cm^3/s)	h_M, mils (mm)
Two-groove cylindrical	35 (19.44)	138 (58.9)	3.58	1.21 (76.7)	0.490 (31.05)	1.23 (0.0312)
Symmetric three-lobe	49 (27.22)	144 (62.2)	4.97	1.22 (77.3)	0.516 (32.7)	0.96 (0.0244)
Canted three-lobe	31 (17.22)	135 (57.2)	5.20	2.01 (127.4)	0.940 (59.6)	1.05 (0.0267)
Tilting-pad	26 (14.44)	134 (56.7)	4.88	2.26 (143.2)	0.311 (19.71)	1.02 (0.0259)

The following values were used: ω = 6000 lb (2721 kg), SAE 20 oil, L = 3 in (76 mm), D = 3 in (76 mm), N = 1800 rpm, t_i = 120°F (48.9°C), c = 0.008 in (0.076 mm).

mechanism for self-excited rotor whirl. Whirl is manifest as an orbiting of the journal at a subsynchronous frequency, usually close to one-half the rotating speed. Whirl is usually destructive and must be avoided.

It is the purpose of this section to provide some insight into bearing dynamics, present some background on analytical methods and representations, and discuss some particular bearings and factors that can influence dynamic characteristics. Dynamic performance data and sample problems are presented for several bearing types.

The Concept of Cross Coupling As mentioned in the opening paragraphs of this subsection, a journal bearing derives load capacity from viscous pumping of the lubricant through a small clearance region. To generate pressure, the resistance to pumping must increase in the direction of the fluid flow. This is accomplished by a movement of the journal such that the clearance distribution takes on the form of a tapered wedge in the direction of rotation, as shown in Figure 1.

The attitude angle γ in Figure 1 is the angle between the load direction and the line of centers. Thus, the displacement of the journal is not along a line that is coincident with the load vector, and a load in one direction causes not only displacements in that direction, but orthogonal displacements as well.

Similarly, a displacement of the journal in the bearing will cause a load opposing the displacement and a load orthogonal to it. Thus, strong cross-coupling influences are introduced by the mechanism by which a bearing operates. The concept of cross-coupling is significant in dynamic characteristics.

It is the cross-coupling characteristics of a journal bearing that can promote self-excited instabilities in the form of bearing whirl. Motion in one direction produces orthogonal forces that in turn cause orthogonal motion. The process continues, and an orbital motion of the journal results. This orbital motion is generally in the same direction as shaft rotation and subsynchronous in frequency. Half-frequency whirl is a self-excited phenomenon and does not require external forces to promote it.

Cross-Coupled Spring and Damping Coefficients For dynamic considerations, a convenient representation of bearing characteristics is a cross-coupled spring and damping coefficients. These are obtained as follows (refer to Figure 1):

1. The equilibrium position to support the given load is established by computer solution of Reynolds' equation.
2. A small displacement to the journal is applied in the y direction. A new solution of Reynolds' equation is obtained, and the resulting forces in the x and y directions are produced. The spring coefficients are as follows:

$$K_{xy} = \frac{\Delta F_x}{\Delta y} \tag{38}$$

$$K_{yy} = \frac{\Delta F_y}{\Delta y} \tag{39}$$

where K_{xy} = the stiffness in the x direction due to y displacement
ΔF_x = the difference in x forces between displaced and equilibrium positions
Δy = the displacement from the equilibrium position in the y direction
K_{yy} = the stiffness in the y direction due to y displacement
ΔF_y = the difference in y forces between displaced and equilibrium positions

3. The journal is returned to its equilibrium position and an x displacement is applied. Similar reasoning produces K_{xx} and K_{yx}.

The cross-coupled damping coefficients are produced in a similiar manner, except, instead of displacements in the x and y direction, velocities in these directions are consecutively applied with the journal in the equilibrium position. The mechanism for increasing the load capacity is squeeze film in which the last term on the right-hand side of

Equation 14 is actuated. Thus, for most fixed bearing configurations, eight coefficients exist: four spring and four damping. The total force on the journal is

$$F_i = K_{ij}x_j + D_{ij}\dot{x}_j \tag{40}$$

where F_i = force in the ith direction.

Repeated subscripts imply the following summation:

$$K_{ij}x_j = K_{ix}x + K_{iy}y + \ \ldots$$

It should be realized that the cross-coupled spring and damping coefficients represent a linearization of bearing characteristics. When they are used, the equilibrium position should be accurately determined, as the coefficients are valid for only a small displacement region encompassing the equilibrium position of the journal. This is true because the spring and damping coefficients remain constant for only a small region of the equilibrium position.

Consider the two-groove cylindrical bearing shown in Figure 1, with the geometric and operating conditions indicated in Table 3. The computer solution (also the performance curves in Figure 13) produces the following results:

Bearing load w = 20,780 lb (9,424 kg)

Power loss = 15.51 hp (11.56 kW)

Minimum film thickness h_M = 0.00125 in (0.032 mm)

Side leakage q_s = 0.941 gpm (3.56 l/mm)

The spring and damping coefficients are

Spring coefficients, lb/in (kg/mm):

$$\begin{bmatrix} K_{xx} & K_{xy} \\ K_{yx} & K_{yy} \end{bmatrix} = \begin{bmatrix} -12.14 \times 10^6 & -4.64 \times 10^6 \\ 28.3 \times 10^6 & -20.41 \times 10^6 \end{bmatrix}$$

Damping coefficients, lb · s/in kg · s/in:

$$\begin{bmatrix} D_{xx} & D_{xy} \\ D_{yx} & D_{yy} \end{bmatrix} = \begin{bmatrix} -2.85 \times 10^4 & 2.66 \times 10^4 \\ -2.69 \times 10^4 & -1.11 \times 10^5 \end{bmatrix}$$

The negative signs imply a positive stiffness because the restoring load is opposite the applied load. Note that for this bearing configuration there is very strong cross-coupling, evidenced by the magnitude of the off-diagonal terms.

Critical Mass The cross-coupled spring and damping coefficients provide a convenient way of representing a bearing in a stability analysis. They reduce the fluid film bearing to a spring-mass system (see Figure 20), and consequently stability and dynamics problems are simplified considerably.

Consider a journal of mass M operating in a bearing. The journal can be considered to have two degrees of freedom, x and y. The governing equations are

TABLE 3 Two-Groove Cylindrical Bearing Geometry and Operating Conditions

Journal diameter D	=	5 in (127 mm)
Bearing length L	=	5 in (127 mm)
Active pad angle θ_p,	=	160° (10° grooves on either side)
Radial clearance c	=	0.0025 in (0.064 mm)
Operating speed N	=	5000 rpm
Lubricant viscosity μ	=	2×10^{-6} lb · s/in^2 (13.79×10^{-3} Pa · s)
Eccentricity ratio ε	=	0.5
Load direction is vertical downward		

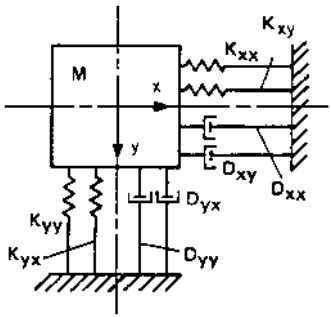

FIGURE 20 Point mass representation of a bearing supported on cross-coupled springs and dampers.

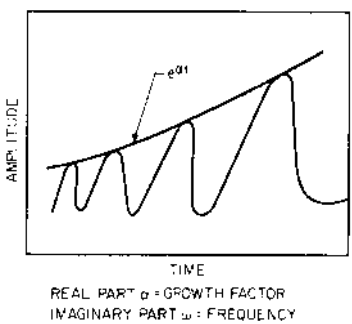

Interpretation of $\chi = \chi_o e^{\beta t}$
where
$\beta = \alpha + i\omega$
$\chi = \chi_o e^{\alpha t} e^{i\omega t} = \chi_o e^{\alpha t}(\text{COS } \omega t + i \sin \omega t)$

FIGURE 21 Interpretation of the growth factor α and orbital frequency ω.

$$M\ddot{x} + D_{xx}\dot{x} + D_{xy}\dot{y} + K_{xx}x + K_{xy}y = 0 \tag{41}$$

$$M\ddot{y} + D_{yy}\dot{y} + D_{yx}\dot{x} + K_{yy}y + K_{yx}x = 0 \tag{42}$$

Assume a sinusoidal response to the form

$$x = x_0 e^{\beta t} \tag{43}$$

$$y = y_0 e^{\beta t} \tag{44}$$

where β is a complex variable:

$$\beta = \alpha + i\omega \tag{45}$$

By the Euler expansion of $e^{\beta t}$, another way to write Equations 43 and 44 is

$$x = x_o e^{\alpha t}(\cos \omega t + i \sin \omega t) \tag{46}$$

$$y = y_o e^{\alpha t}(\cos \omega t + i \sin \omega t) \tag{47}$$

An interpretation of α and ω is shown in Figure 21. The real part of $\beta = \alpha$ is called the *growth* or *attenuation factor*. The imaginary part is the frequency of vibration. A positive real part means that the response to a disturbance grows in time. The growth factor is similar to the logarithmic mean decrement, which is common in vibration theory:

$$\alpha\tau = \ln \frac{x_{n+1}}{x_n} \tag{48}$$

where τ = period of vibration
x_{n+1} = amplitude at time $n + 1$
x_n = amplitude at time n

Thus, the growth factor α is a measure of the growth or decay of the journal to a small disturbance. A positive growth factor implies an instability.

The solutions to Equations 41 and 42 are obtained by substituting Equations 43 and 44, which produces the following:

$$\begin{bmatrix} (M\beta^2 + D_{xx}\beta + K_{xx}) & (D_{xy}\beta + K_{xy}) \\ (\beta D_{yx} + K_{yx}) & (M\beta^2 + \beta D_{yy} + K_{yy}) \end{bmatrix} \begin{Bmatrix} x_0 \\ y_0 \end{Bmatrix} = \{0\}$$

To obtain a solution, the determinant of the coefficient matrix must vanish. Expansion produces a polynomial in β that can be solved for the roots of β, which in turn provide the growth factors and frequencies of vibration.

It is possible to obtain a closed-form solution of Equations 41 and 42 for the critical mass and resulting orbital frequency. The critical mass M is defined as that mass above which an instability will occur. At the threshold of instability, the real part of $\beta = \alpha$ goes to zero and $\beta = i\omega$.

Substituting into Equation 49, expanding the determinant and separating real and imaginary components produces the following equations:

$$M^2\omega^4 - \underbrace{M(K_{yy} + K_{xx})}_{A}\omega^2 + \underbrace{(D_{yx}D_{xy} - D_{xx}D_{yy})}_{B}\omega^2 + \underbrace{K_{xx}K_{yy} - K_{xy}K_{yx}}_{C} = 0 \tag{50}$$

$$\underbrace{M(D_{yy} + D_{xx})}_{D}\omega^2 + \underbrace{(D_{xy}K_{yx} + D_{yx}K_{xy} - D_{xx}K_{yy} - D_{yy}K_{xx})}_{E} = 0 \tag{51}$$

The two equations can be solved for M and ω:

$$M = \frac{BED}{E^2 - AED + CD^2} \tag{52}$$

$$\omega = \sqrt{\frac{-(AED + E^2 + CD^2)}{BD^2}} \tag{53}$$

Thus, if the cross-coupled coefficients are known, it is possible to determine the critical mass and the orbital frequency. If the mass acting on the bearing exceeds or equals the critical value, then an instability will occur.

Dynamic Stability of Various Bearing Types Several parameters can be used to establish the stability characteristics of a particular type of bearing. The most significant is the critical mass, derived above. It is also possible to get some feel for stability from purely steady-state performances by examining the bearing attitude angle. The larger the attitude angle, the greater the cross-coupling influence and the worse the stability characteristics. Interpreting attitude angles, however, can prove misleading.

Figure 22 shows plots of the attitude angle γ versus the load parameter W for some of the different types of bearings previously described. The contradiction in these results is that the symmetric three-lobe bearing has higher attitude angles than the two-groove cylindrical bearing even though, as will be subsequently demonstrated, it has superior stability characteristics. The reason for the higher attitude angle is that the bearing is cavitating in the diverging region of the loaded pad, which results in a large shift in the journal. Whirl motion, however, is prevented by the accompanying lobes.

A more direct and accurate approach to establishing bearing stability is to determine the critical mass acting on the bearing. Figure 23 shows the results obtained for the fixed

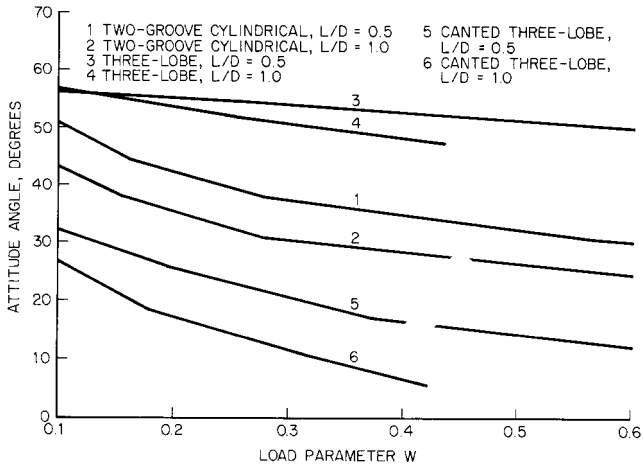

FIGURE 22 Attitude angle versus load parameter for various bearing types.

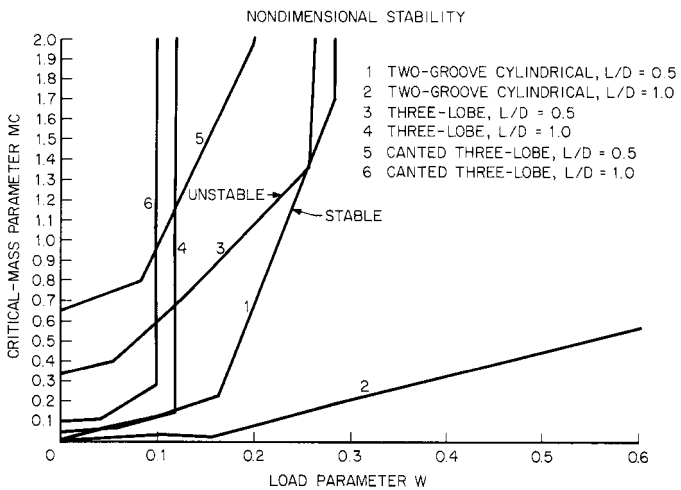

FIGURE 23 Critical mass versus load parameter for various bearing types.

bearing geometries previously discussed. For any particular bearing geometry, if the critical mass attributable to the bearing exceeds that of the data plotted, the bearing will be unstable. Thus, if the plotted point falls to the right of the bearing line, the bearing is stable; if it falls to the left, the bearing is unstable.

The critical mass is defined as follows:

$$M = m\omega Rc^3/24\mu L^5 \tag{54}$$

where M = nondimensional critical mass
m = dimensional critical mass, lb · s²/in (kg · s²/mm)
ω = shaft speed, rad/s
R = shaft radius, in (mm)
c = bearing machined radial clearance, in (mm)
μ = lubricant viscosity, lb sec/in² (Pa · s)
L = bearing length, in (mm)

An examination of the curves in Figure 23 clearly indicates the superiority of the canted three-lobe bearing and the inferiority of the cylindrical configuration.

EXAMPLE Consider a high-speed bearing for which

N = 60,000 rpm
ω = 60,000π/30=6283 rad/s
D = 1 in (25.4 mm)
L = 0.5 in (12.7 mm)
$\mu = 1\times10^{-6}$ lb · s/in^5 (6.9 x 10^{-3} Pa · s)
C = 0.0005 in (0.013 mm)
w = 100 lb (45.35 kg)

$$W = \frac{wC^2}{6\mu\omega RL^3} = \frac{(100)(0.0005^2)}{(6)(1\times10^{-6})(6283)(0.5)(0.5^3)} = 0.0106$$

The value of M is obtained from Figure 22 and indicated in Table 4 for the various bearing types considered. Dimensional units are also given. Table 4 clearly indicates that the lobe bearings can permit significantly more attributable mass than the cylindrical bearing can. If a symmetric rotor is being supported by two bearings, the cylindrical bearings would be unstable if half the weight of the rotor exceeded 14.7 lb (6.67 kg). The half weights go to 258 lb (117 kg) and 501 lb (227.2 kg) for the symmetric three-lobe and canted three-lobe bearings, respectively. No mention has been made of the tilting-pad bearing because, for all practical purposes, these bearings are always stable.

OPERATING CONDITIONS THAT AFFECT BEARING STABILITY

Cavitation Figure 1 shows a pressure distribution in a journal bearing. Positive pressure is generated in the converging wedge because the journal is pumping fluid through a restriction. On the downstream side of the minimum film thickness, the journal is pumping fluid out of a diverging region. In this region, the pressure decreases. Either the pressure becomes negative, which is defined as pressure below the ambient pressure,

TABLE 4 Stability Comparison Chart

Bearing type	M	m, lb · s²/in (kg · s²/mm)	w', lb (kg)[a]
Two-groove cylindrical	0.02	0.038 (6.79 × 10^{-4})	14.7 (6.7)
Symmetric three-lobe	0.85	0.668 (11.9 × 10^{-3})	257.9 (117.1)
Canted three-lobe	0.68	1.299 (23.2 > 10^{-3})	501.4 (227.6)
	$m = \frac{24M\mu h^5}{\omega Rc^3} = \frac{M(24)(10^{-6})(0.5^5)}{(6283)(0.5)(0.0005^3)} = 1.91M$		

[a]The w' represents the maximum mass in weight units that could act on the bearing.

or the film cavitates and decreases to atmospheric pressure as the lubricant releases entrapped air.

With respect to stability, cavitation is a more desirable condition than the development of negative pressure. From an examination of Figure 1, it can be seen that the negative pressure pulls the journal in an orthogonal direction and increases the cross-coupling. The more eccentric the bearing, the larger the negative pressure or cavitated region.

In lightly loaded bearings that are pressure-fed, negative pressures can occur because pressures in the divergent region have not approached atmospheric pressure. Cavitation does not occur, and the bearing is prone to instability. Thus, the feed pressure and load on a bearing are two additional parameters that affect stability.

Lobe bearings are often used because of their excellent antiwhirl characteristics. Figure 9 earlier showed two types of lobe bearings: symmetric and canted. The symmetric lobe bearing is designed so that, in the concentric position, the minimum film thickness occurs at the center of each lobe. Note that this permits a region of converging film followed by a region of diverging film. Thus, depending upon the ambient pressure, it is possible to have negative pressures in a symmetric lobe bearing. Under very high ambient conditions, a symmetric lobe bearing can go unstable.

The canted lobe bearing is designed to have a completely converging wedge and positive pressure throughout its arc length. Its stability characteristics are superior to those of the symmetric lobe bearing. Its steady-state characteristics are also superior.

Hybrid Bearings At times, externally pressurized bearings are resorted to for stability improvements. The philosophy is that externally pressurized bearings are not subject to high attitude angles, as is the case with hydrodynamic journal bearings. Although this is generally true, hybrid hearings can still be subject to considerable cross-coupling. Figure 11 showed a schematic arrangement of a hybrid bearing. Oil is fed through restrictors from an external source into pocket recesses. From there, it exits into the clearance region between recesses. Lubricant is also pumped into and out of recesses by the rotating shaft by a viscous drag in the same manner as with a purely hydrodynamic bearing.

Consider recess 2 in Figure 11. Oil is pumped from the shaft via a converging wedge, and it augments the pressure in the recess provided by the external system. The net result is a higher pressure in the bearing domain covered by recess 2 than would occur without rotation. Now consider recess 3. Here the journal is pumping fluid out of the recess into a diverging film, so that the hydrodynamic action tends to reduce the pressure in this recess domain. By similar reasoning, it can be shown that recess 4 operates at a lower pressure than recess 1. The net result of these variations in pressure due to rotation is that cross-coupling forces are introduced and the hybrid bearing may not prevent instability.

BEARING MATERIALS AND FAILURE MODES

Materials The most common material used for oil-lubricated fluid film bearings is babbitt. Tin- and lead-based babbitts are relatively soft materials and offer the best insurance against shaft damage. They also enable embedded dirt and contaminants without significant damage.

Two types of babbitts are in common use. One has a tin base (86 to 88 percent), with about three to eight percent copper and four to 14 percent antimony. The other has a lead base with a maximum of 20 percent tin and about 10 to 15 percent antimony. The remainder is principally lead. The physical properties of babbitt are shown in Table 5. The primary limitations of babbitt are operating temperature (300°F [140°C] max) and fatigue strength. The chemical composition of various babbitt alloys are indicated in Table 6.

Tin-based babbitts have better characteristics than lead-based babbitts; they have better corrosion resistance, are less likely to wipe under poor conditions of lubrication, and can be bonded more easily than lead-based materials. Because of cost considerations, however, lead-based babbitts are widely used. The more widely used is the SAE 15 alloy containing one percent arsenic (refer to Table 6).

TABLE 5 Properties of Bearing Alloys

Bearing material	Brinell hardness at room temperature	Brinell hardness at 30°F (17°F)	Minimum Brinell hardness of shaft	Load carrying capacity, lb/in^2 (kg/m^2)	Max operating temperature, °F (°C)
Tin-based babbitt	20–30	6–12	150 or less	800–1500 (5.62×10^5 – 10.55×10^5)	300 (149)
Lead-based babbitt	15–20	6–12	150 or less	800–1200 (5.62×10^5 – 8.44×10^5)	300 (149)

SOURCE: Ref. 8

TABLE 6 Composition[a] Percentages of Babbitts with SAE Classifications of 11 to 15

Element	SAE No. (Similar ASTM Spec.)				
	11 (None)	12 (B23, alloy 2)	13 (None)	14 (B23, alloy 7)	15 (B23, alloy 15)
Tin (mm)	86.0	88.2	5.0–7.0	9.2–10.8	0.9–1.2
Antimony	6.0–7.5	7.0–8.0	9.0–11.0	14.0–16.0	14.0–15.5
Lead	0.5	0.5	Remainder	Remainder	Remainder
Copper	5.0–6.5	3.0–4.0	0.5	0.5	0.5
Iron	0.08	0.08	—	—	—
Arsenic	0.1	0.1	0.25	0.6	0.8-1.2
Bismuth	0.08	0.08	—	—	—
Zinc	0.005	0.005	0.005	0.005	0.005
Aluminum	0.005	0.005	0.005	0.005	0.005
Cadmium	—	—	0.05	0.05	0.05
Others	0.2	0.2	0.2	0.2	0.2

[a]The percentage of minor constituents represents limiting values except as noted.
SOURCE: *SAE Handbook,* Society of Automotive Engineers. New York, 1960, p. 201.

Tin-based babbitts do not experience as many corrosion problems as lead-based babbitts. SAE 11 babbitts (containing eight percent antimony and eight percent copper) are used extensively for industrial applications.

Babbitts are bonded to a backing shell of another material, such as steel or bronze, because they are not a good structural material. The thinner the babbitt layer, the greater the fatigue resistance. In automotive applications where resistance to fatigue is important, babbitt thickness is from 0.001 to 0.005 in (0.02 to 0.12 mm). For pump applications, the thickness varies from $\frac{1}{32}$ to $\frac{1}{8}$ in (0.8 to 3 mm). The thicker layers provide good conformity and embedability.

Failure Modes The failure modes most commonly found are fatigue, wiping, overheating, corrosion, and wear.

Fatigue occurs because of cyclic loads normal to the bearing surface. Figure 24 shows babbitt fatigue in a 7-in (178-mm) diameter journal bearing from a steam turbine.

Wiping results from surface-to-surface contact and smears the babbitt, as shown in Figure 25. The usual causes of wiping are a bearing overload, insufficient rotational speed to form a film, and loss of lubricant.

FIGURE 24 Babbitt fatigue in a 7-in (178-mm) diameter turbine bearing. (Westinghouse Electric Corp. *Photo originally reproduced in* Ref. 8, p.18–19.)

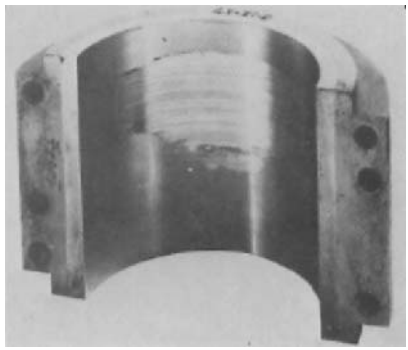

FIGURE 25 Bearing wipe on a 3-in (76-mm) diameter bearing due to temporary loss of lubricant. (Westinghouse Electric Corp. *Photo originally reproduced in* Ref. 8, p.18–25)

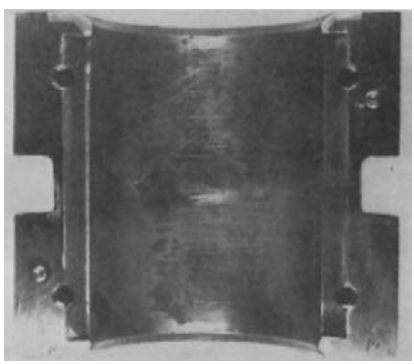

FIGURE 26 Corrosion on a 5-in (127-mm) diameter, lead-based babbitt bearing. (Westinghouse Electric Corp. *Photo originally reproduced in* Ref. 8, p. 18–21)

Overheating is manifest by discoloration of the surface and cracking of the babbitt material. Corrosion is failure by a chemical action. It is more common with lead-based babbits, which react with acids in the lubricant. Figure 26 shows corrosion damage for a 5-in (127-mm) diameter, lead-based babbitt bearing.

Wear results from contaminants in the film and is evidenced by scoring marks that may be localized or persist around a large circumferential region of the bearing.

REFERENCES

[1]Fuller, D. D. *Theory and Practice of Lubrication for Engineers*. Wiley, New York, 1956.

[2]Castelli, V. and W. Shapiro. "Improved Method of Numerical Solution of the General Incompressible Fluid-Film Lubrication Problem." *Trans. ASME, J. Lub. Technol.,* April, 1967, pp. 211–218.

[3]Castelli, V.,and J. Pirvics. "Review of Methods in Gas-Bearing Film Analysis." *Trans. ASME, J. Lub. Technol.,* October 1968, pp. 777–792.

[4]Pinkus, O. and B. Sternlicht. *Theory of Hydrodynamic Lubrication*. McGraw-Hill, New York, 1961.

[5]Ng, C. W. and C. H. T. Pan. "A Linearized Turbulent Lubrication Theory." *Trans. ASME, J. Basic Eng.,* Series D, Vol. 87, 1965, p. 675.

[6]Elrod, H. G. and C. W. Ng. "A Theory for Turbulent Films and Its Application to Bearings." *Trans. ASME, J. Lub. Technol.,* July 1967, p. 346.

[7]Shapiro, W., and R. Colsher. "Dynamic Characteristics of Fluid Film Bearings." *Proc. Sixth Turbomachinery Symposium,* sponsored by the Gas Turbine Laboratories, Department of Mechanical Engineering, Texas A&M University, College Station, Texas, December 1977.

[8]O'Connor, J. I., J Boyd, and E. A. Avallone. *Standard Handbook of Lubrication Engineering*. McGraw-Hill, New York, 1968.